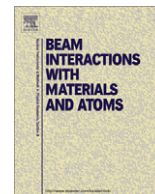




Contents lists available at SciVerse ScienceDirect

## Nuclear Instruments and Methods in Physics Research B

journal homepage: [www.elsevier.com/locate/nimb](http://www.elsevier.com/locate/nimb)

## Synthesis and characterisation of copper doped Ca–Li hydroxyapatite

M.A. Pogosova<sup>a,\*</sup>, P.E. Kazin<sup>a</sup>, Y.D. Tretyakov<sup>b</sup><sup>a</sup> Department of Chemistry, Lomonosov Moscow State University, Leninskie Gory 1 (3), 119991 Moscow, Russian Federation<sup>b</sup> Department of Material Science, Lomonosov Moscow State University, Leninskie Gory 1 (73), 119991 Moscow, Russian Federation

## ARTICLE INFO

Article history:  
Available online xxxKeywords:  
Hydroxyapatite  
Pigment

## ABSTRACT

Hydroxyapatites  $M_{10}(PO_4)_6(OH)_2$  (MHAP), where M is an alkaline earth metal, colored by incorporation of copper ions substituting protons, were discovered recently [1]. Now this kind of apatite-type materials can be used as inorganic pigments. Until now blue (BaHAP), violet (SrHAP) and wine-red (CaHAP) colors were achieved by the copper ions introduction [2]. The task of the present work was to study possibility of further M-ion substitution to affect the color and shift it toward the red–orange tint. Polycrystalline hydroxyapatites  $Ca_{10-x}Li_xCu_z(PO_4)_6O_2H_{2-y-z-\sigma}$  (Ca–LiHAP) were synthesized by solid state reaction at 1150 °C (ceramic method) and studied by X-ray powder diffraction (XRD), infrared absorption and diffuse-reflectance spectroscopy. Refinement of the X-ray diffraction patterns by the Rietveld method shows that CaHAP unit cell parameters are a little bigger, than Ca–LiHAP ones. Small difference between unit cell parameters could be caused by two ways of the  $Li^+$  ions introduction: (1) at the  $Ca^{2+}$  sites (Ca–Li substitution); (2) into hexagonal channels (H–Li substitution). The Li ions doping changes the color of the copper doped CaHAP from wine-red to pink and red.

© 2011 Elsevier B.V. All rights reserved.

## 1. Introduction

Apatite-type materials are well-known as biomimetic materials [3], sorbents of toxic components [4,5], catalysts for such important industrial reactions as conversion of methane, dehydration of alcohol, etc. [6,7]. Specific properties were achieved by cation or/and anion substitution. In [1] it was found that copper ions doping could change the color of  $Sr_5(PO_4)_3OH$  (SrHAP) from white to violet. Now this material is used as an inorganic pigment with excellent characteristics (intense color, weather stable, antifungal effect, etc.) [8]. Soon after SrHAP, the copper doped and colored BaHAP (blue) and CaHAP (wine-red) were obtained [2]. Thus, the decrease of the metal ion size in Ba–Sr–Ca line changes the color spectra from blue to red zone. The quantity of doped copper ions has an influence on the color intensity. The XRD with refinements by the Rietveld method showed, that the copper ions were introduced to the hexagonal channels of the apatite structure (Fig. 1). But the reason of color appearance is still not completely clear. But the only fact we know is that the color is depending on unit cell parameters. So is it possible to achieve red, orange or yellow color by the further unit cell parameters decrease? A big part of manufactured yellow pigments are based on Pb or Cd compounds. It means that they contain a king of high polluting components. Therefore it is important to search for the alternative yellow–red pigments. Copper is not so poisoning compared with Pb and Cd.

Furthermore, only small quantities of copper are needed for the intense colored apatite (index z is less than 0.4). Substitution of Li for Ca has been chosen for this purpose.

## 2. Experimental

As starting reagents for CaHAP synthesis  $CaCO_3$ ,  $(NH_4)_2SO_4$ ,  $(NH_4)_2HPO_4$ ,  $Li_2CO_3$ , and CuO were used (99.9% grade). Five series of different HAP's and one model series were prepared (Table 1) with  $z = 0, 0.1$  and  $0.3$  and different Ca/Li ratios. All the reagents were mixed and ground in a agate mortar, followed by successive annealing steps in alumina crucibles at 600 °C for 1 h and at 800 °C for 3 h. Then the samples were annealed at 1150 °C for 3 h for two times. Finally, they were pressed into pellets and annealed at 1150 °C for 3 h (target samples). Preliminary studies showed that further annealing of the powder does not change the phase composition of the target samples. The samples were cooled on air after each heat treatment step. Furthermore, the synthesis was performed with intermittent grindings and XRD analysis after each annealing treatment. XRD patterns of  $Ca_{5.2}Li_1(PO_4)_3Cu_xOH_{1-x-\delta}$ ,  $x = 0.3$  (PM10) and  $Ca_{5.2}(PO_4)_3Cu_xOH_{1-x-\delta}$ ,  $x = 0.3$  (PM Model 3) after the first, second and last step of the annealing process are shown on Fig. 2.

Phase composition of the synthesized samples was determined by X-ray powder diffraction analysis (XRD) using the Guinie system FR-552 (with Ge standard and Cu  $K_{\alpha 1}$  radiation). The XRD of target samples was measured on a Rigaku diffractometer (with Cu  $K_{\alpha}$  radiation and  $2\theta$  range from 5 to 80°) and were analyzed by

\* Corresponding author.

E-mail address: [nanaika-muse-999@yandex.ru](mailto:nanaika-muse-999@yandex.ru) (M.A. Pogosova).

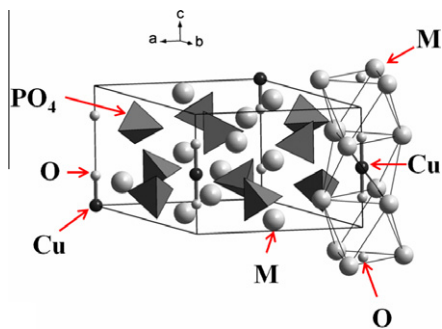


Fig. 1. Copper doped apatite structure.

the Rietveld procedure with program Jana2006. By these investigations the phase transformation after each step were controlled and the unit cell parameters of the target samples were determined. Two equilibrium, stable and pure phases were obtained in the third and fifth series (Table 1). These samples were analyzed by diffuse-reflectance spectroscopy using Perkin Elmer Lambda 950 (with scanning range from 150 to 1170 nm); IR method, using Perkin Elmer Spectrum One (with scanning range from 4000 to 450  $\text{cm}^{-1}$ ).

### 3. Results and discussion

#### 3.1. X-ray powder diffraction

Our preliminary study (first two sample series) showed that  $\text{SO}_4$  group was not incorporated into the apatite structure. Furthermore, decrease of calcium content causes the decrease of the apatite phase content (Table 1). Taking into consideration these results, Ca/Li ratios were corrected and the last three series were prepared. Two of them (third and fifth) contain pure apatite phase with different unit cell parameters (Table 2). Small difference between the unit cell parameters of CaLiHAPs and the model samples (without Li) could be caused by two ways of  $\text{Li}^+$  ions introduction:

- (1) substitution of Ca, that reduce the cell parameters – cause the more red color;
- (2) incorporation into the hexagonal channels, that increase the cell parameters;

**Table 1**  
Phase composition of the synthesized samples determined by X-ray powder diffraction analysis.

Series No.	Sample, nominal composition	Phase composition
0	PM0 $\text{Ca}_4\text{Li}(\text{PO}_4)_2(\text{SO}_4)\text{OH}$ PM0Cu	≈60% of the apatite phase. $\text{SO}_4$ group didn't placed into the apatite structure
1	PM1 $\text{Ca}_{4.5}\text{Li}_{0.5}(\text{PO}_4)_3(\text{OH})_{0.5}$ PM1Cu	≈100% of $\text{Ca}_5\text{Li}_{0.5}(\text{PO}_4)_{3.5}$ phase
2	PM3 $\text{Ca}_5(\text{PO}_4)_3\text{Li}_{0.5}\text{OH}_{0.5}$ PM3Cu	≈70% of the apatite phase
3	PM8 $\text{Ca}_{5.2}\text{Li}_{0.3}(\text{PO}_4)_3$ PM9 $\text{Ca}_{5.2}\text{Li}_{0.3}(\text{PO}_4)_3\text{Cu}_{0.1}$ PM10 $\text{Ca}_{5.2}\text{Li}_{0.3}(\text{PO}_4)_3\text{Cu}_{0.3}$	100% of the apatite phase
4	PM11 $\text{Ca}_{5.3}\text{Li}_{0.2}(\text{PO}_4)_3$ PM12 $\text{Ca}_{5.3}\text{Li}_{0.2}(\text{PO}_4)_3\text{Cu}_{0.1}$ PM13 $\text{Ca}_{5.3}\text{Li}_{0.2}(\text{PO}_4)_3\text{Cu}_{0.3}$	≈100% of the apatite phase. Negligible quantities of CaO
5	PM26 $\text{Ca}_{5.2}\text{Li}_1(\text{PO}_4)_3$ PM27 $\text{Ca}_{5.2}\text{Li}_1(\text{PO}_4)_3\text{Cu}_{0.1}$ PM28 $\text{Ca}_{5.2}\text{Li}_1(\text{PO}_4)_3\text{Cu}_{0.3}$	100% of the apatite phase
Model	PM Model 1 $\text{Ca}_5(\text{PO}_4)_3\text{OH}$ PM Model 2 $\text{Ca}_5(\text{PO}_4)_3\text{Cu}_{0.1}$ PM Model 3 $\text{Ca}_5(\text{PO}_4)_3\text{Cu}_{0.3}$	100% of the apatite phase

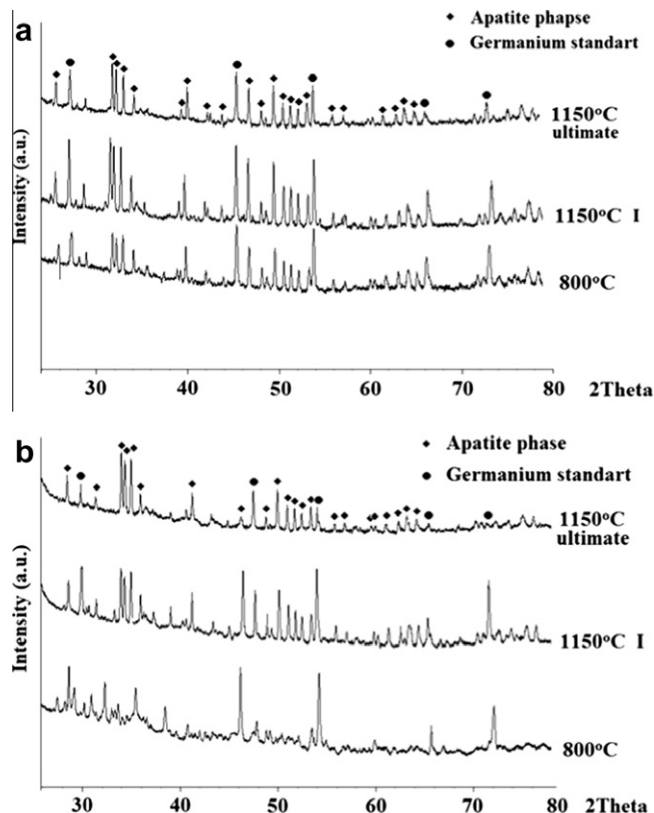


Fig. 2. XRD patterns of: (a)  $\text{Ca}_{5.2}\text{Li}_1(\text{PO}_4)_3\text{Cu}_x\text{OH}_{1-x-\delta}$ ,  $x = 0.3$  (PM10); (b)  $\text{Ca}_{5.2}(\text{PO}_4)_3\text{Cu}_x\text{OH}_{1-x-\delta}$ ,  $x = 0.3$  (PM Model 3). Pattern marked with "I" symbol is a diagram of the sample after the first annealing at 1150 °C.

**Table 2**  
Unit cell parameters refined using the Rietveld method.

Series No.	Sample	$a/\text{Å}$	$c/\text{Å}$	$V/\text{Å}^3$
3	PM8 $\text{Ca}_{5.2}\text{Li}_{0.3}(\text{PO}_4)_3$	9.415(1)	6.880(1)	528.1(1)
	PM9 $\text{Ca}_{5.2}\text{Li}_{0.3}(\text{PO}_4)_3\text{Cu}_{0.1}$	9.423(1)	6.887(1)	529.7(1)
	PM10 $\text{Ca}_{5.2}\text{Li}_{0.3}(\text{PO}_4)_3\text{Cu}_{0.3}$	9.432(1)	6.903(1)	531.8(1)
5	PM26 $\text{Ca}_{5.2}\text{Li}_1(\text{PO}_4)_3$	9.417(1)	6.884(1)	528.7(1)
	PM27 $\text{Ca}_{5.2}\text{Li}_1(\text{PO}_4)_3\text{Cu}_{0.1}$	9.429(2)	6.885(2)	530.1(2)
	PM28 $\text{Ca}_{5.2}\text{Li}_1(\text{PO}_4)_3\text{Cu}_{0.3}$	9.436(1)	6.906(2)	532.5(1)
Model	PM Model 1 $\text{Ca}_5(\text{PO}_4)_3\text{OH}$	9.419(2)	6.879(2)	528.5(2)
	PM Model 2 $\text{Ca}_5(\text{PO}_4)_3\text{OH}_{0.5}\text{Cu}_{0.1}$	9.424(3)	6.890(3)	530.0(2)
	PM Model 3 $\text{Ca}_5(\text{PO}_4)_3\text{OH}_{0.7}\text{Cu}_{0.3}$	9.443(3)	6.903(5)	533.0(3)

#### 3.2. Diffuse-reflectance spectroscopy

Colored samples of model CaHAP and samples of CaLiHAPs exhibit a difference in the reflectance in the region between 380 and 600 nm. The peak between 380 and 430 nm, that adds the yellow tint, is bigger in CaLiHAP's samples. Yellow component of the color causes more red and light color of the Li-doped samples.

#### 3.3. Infrared spectroscopy

Infrared spectra of substituted phosphate hydroxyapatite  $\text{Ca}_{5.2}\text{Li}_{0.3}(\text{PO}_4)_3\text{Cu}_x\text{OH}_{1-x-\delta}$  and  $\text{Ca}_{5.2}\text{Li}_1(\text{PO}_4)_3\text{Cu}_x\text{OH}_{1-x-\delta}$ ,  $x = 0, 0.1, 0.3$  are shown in Fig. 3. Wide intense bands in the 1200–950 and 600–450  $\text{cm}^{-1}$  regions can be assigned to vibrations of  $(\text{PO}_4)^{3-}$  ions. Bands in the region of 3570 and 640  $\text{cm}^{-1}$  are due to the stretching and libration modes of the  $\text{OH}^-$  groups. Fig. 2 shows that the bands of the  $\text{OH}^-$  libration and stretching modes

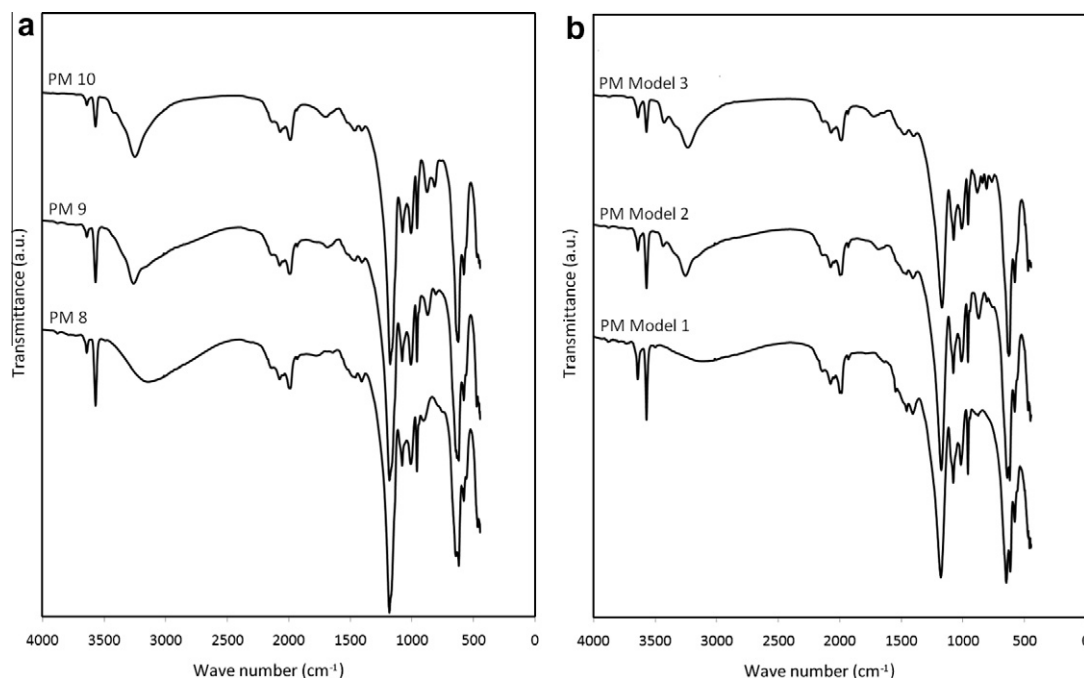


**Fig. 3.** Infrared spectra of the samples: (a)  $\text{Ca}_{5.2}\text{Li}_{0.3}(\text{PO}_4)_3\text{Cu}_x\text{OH}_{1-x-\delta}$ ,  $x = 0$  (PM8); 0.1 (PM9); 0.3 (PM10); (b)  $\text{Ca}_{5.2}(\text{PO}_4)_3\text{Cu}_x\text{OH}_{1-x-\delta}$ ,  $x = 0$  (PM Model 1); 0.1 (PM Model 2); 0.3 (PM Model 3).

become less intense with increasing Cu substitution. Additional absorption between  $900\text{--}750\text{ cm}^{-1}$  is due to a vibration of the Cu–O. There is some difference between CaLiHAP and CaHAP in this range. Possibly, it could be caused by the Li ion influence and different copper ion's environment.

#### 4. Conclusions

New kinds of apatite-type material was obtained:  $\text{Ca}_{5.2}\text{Li}_{0.3}(\text{PO}_4)_3\text{Cu}_x\text{OH}_{1-x-\delta}$  and  $\text{Ca}_{5.2}\text{Li}_1(\text{PO}_4)_3\text{Cu}_x\text{OH}_{1-x-\delta}$ ,  $x = 0, 0.1, 0.3$ .

Increase of the unit cell's parameters could be caused by the copper and lithium ions introduction into the hexagonal channels. Decrease by the Ca–Li and, possibly, Ca–Cu substitution.

Samples with Li and Cu ions were pale-colored compared with the corresponding Cu-containing samples without Li.

#### References

- [1] P.E. Kazin, A.S. Karpov, M. Jansen, et al., *Z. Anorg. Allg. Chem.* 629 (2003) 344.
- [2] A.S. Karpov, J. Nuss, M. Jansen, P.E. Kazin, Yu.D. Tretyakov, *Solid State Sci.* 5 (2003) 1277.
- [3] D.G. Shchukin, G.B. Sukhorukov, H. Mohwald, *Chem. Mater.* 15 (2003) 3947–3950.
- [4] S. Meski, S. Ziani, H. Khireddine, *J. Chem. Eng. Data* 55 (2010) 3923–3928.
- [5] M. Srinivasan, C. Oferraris, T. White, *Environ. Sci. Technol.* 40 (2006) 7054–7059.
- [6] Z. Boukha, M. Kacimi, M. Fernando, R. Pereira, J. Faria, J. Figueiredo, M. Ziyad, *Applied Catalysis A* 317 (2007) 299–309.
- [7] K. Kaneda, T. Mizugaki, *Energy Environ. Sci.* 2 (2009) 655–673.
- [8] [www.ferro.com](http://www.ferro.com).